INVESTIGATION OF A QUANTIFIED SOUND PROBE FOR STUD WELD QUALITY MEASUREMENT WITH NUMERICAL SIMULATION DATA

Maximilian Rohe[1], Dr. Jörg Hildebrand[1], Prof. Jean Pierre Bergmann[1]

[1]Technische Universität Ilmenau, Ilmenau, Group Production Technology, Ilmenau, Germany
maximilian.rohe@tu-ilmenau.de

ABSTRACT

Drawn arc stud welding with ceramic ferrules is a widely used joining process for joining sheet metal to studs, which can be threaded or sheared. During the welding process, various irregularities can occur which adversely affect the resulting mechanical properties. Arc blowing is one of the most common process defects. Arc blowing can result in an asymmetric weld bead which can increase the failure rate of the stud. An approach to stud testing is given in DIN ISO EN 14555. A sound probe carried out by an experienced welder provides qualitative information about the weld bead. The sound probe causes the stud to vibrate at its natural frequencies. If the eigenfrequencies can be calculated for each weld bead shape, the sound probe can be quantified. To this end, a new simulation approach is presented which allows the rapid calculation of the eigenfrequencies of the stud with different weld bead shapes. A data set is also generated and analyzed.

Index Terms - Stud welding, numerical simulation, modal analysis, welding, sound probe, vibration

1. INTRODUCTION

Drawn arc stud welding with ceramic ferrule is a welding process that joins a stud with a metal substrate by melting the tip of the stud and a small spot on the substrate with an arc. By moving the current-carrying stud up the arc is ignited. The melt pool is formed and by pushing the stud towards the substrate the joining is performed [1]. Furthermore, the melting pool is protected from the environment by a ceramic ferrule, which additionally forms the weld bead. The stud can have different dimensions in the range between 3 mm up to 25 mm in diameter and different lengths. Also, the shape and material can vary depending on the use case like studs with threads or shear connectors. Due to the speed and flexibility of the presented process it is often used in structural engineering as well as in mechanical engineering. Since the stud builds up a magnetic field inducted by the flowing current, the arc can be deflected, and an asymmetric weld bead is produced (Figure 1). The magnetic arc blowing depends on the position of the stud on the substrate and the electrical circuit between the welding machine, stud, and substrate. Those asymmetric welds can negatively affect the strength of the weld and cause rework of the welding.

To check the quality of a stud weld DIN ISO EN 14555 [2] defines different approaches which include destructive testing like bending tests or tensile test. Moreover, there are non-destructive tests like x-ray investigations. Those test procedures are often performed on special specimens but not on the to be welded part.

In addition, Dong et al. [3] developed a methodology for ultrasonic inspection of stud welds. By step scanning the back of the plate where the stud is welded on, a cross-sectional image can be generated. They used A-scans and decomposed the echo signals with using wavelets. Using the frequency representation of the signal they found that the 5.5 MHz response can be used to characterize and measure the weld bead, particularly the weak zone, where the fusion zone is not fully formed. In a similar way to X-ray inspection, it is often only possible to inspect specific samples here due to the limitations of the accessibility. To control every welded stud new approaches are developed using the process parameters like the arc current or voltage to predict the weld bead quality [4–7].
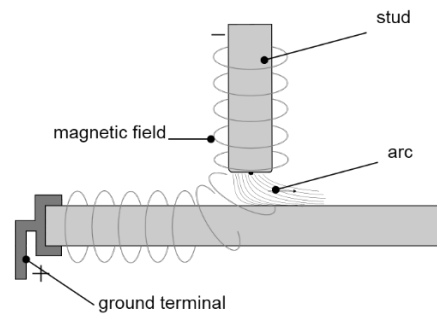

Figure 1: Schematic illustration of the stud welding process with the magnetic field inducted by the current flow

While Samardžić et al. [6,7] used classical statistical features on the current and voltage which are recorded during the welding process, Al Sahib et al. and Naddaf et al.[4,5] used machine learning algorithms to evaluate the weld quality. They all derived other features from the current and voltage, such as resistance or power. The lift of the stud during the welding is also a feature. They found that irregularities in the signals were an indication of defects in the weld.

Independent Component Analysis (ICA) increases the size of the data set to provide more training data. Creating synthetic data gives better results with neural networks, which are used to classify the recorded signals. With known process variations such as contamination of the weld surfaces, six classes can be derived. When testing different neural network architectures such as ResNet, Encoder or classic multi-layer perceptron, the Encoder model showed the best results with an F1 score of 0.84 [5].

The non-destructive approaches presented show good results for general defects in the weld zone or process irregularities that can lead to weld bead defects. However, they are either limited to special cases where there is sufficient space to use the necessary equipment or are not covered by any standard. Arc blowing and in consequence an irregular weld bead shape is also not fully investigated in the approaches presented.

A feasible proposal could be a sound probe which is also mentioned in [2]. The test can only be performed by an experienced welder. Here the welder hits the stud by a hammer and is analyzing the emitted sound qualitative. This process is highly subjective and different welders may classify welds differently which can lead to high error rates [8].

When a stud is struck by the hammer it will vibrate at its eigenfrequencies. In order to quantify the probe test, it is assumed that for asymmetric beads the eigenfrequencies will vary in a specific way so that the change in eigenfrequency can be used to infer the shape of the weld bead. To this end, a simulation model will be developed which is capable of providing information on the eigenfrequencies of different welded studs with different weld bead shapes. If it is possible to generate a sufficient amount of data reflecting possible real-world welds in a reasonable amount of time, the data can be used to develop other methods of recording the vibrations of the stud after hammering and predicting the weld bead shape and hence the arc blow direction.

2. MODELLING OF THE STUD

In this study a head stud is used which is derived from the DIN ISO 13918 [9]. A real-world weld is shown in Figure 2 a). He has a length of 126 mm, and the diameter of the stud is 16 mm. The head has a diameter of 32 mm. As a result of the manufacturing process, there were rounded corners on the edges of the stud. The material of the stud is set to S235J2. As a result of the weld process a weld bead is formed. To secure the bead from the atmosphere and to get the bead in an appropriate shape a ceramic ferrule is used during welding. With a maximal height of 8 mm and a maximal diameter of 20 mm the ferrule is placed on the stud and is broken after successful joining the stud with the underlying metal sheet. The shaped weld seam has an irregular height as well as width. To get the eigenfrequencies of the stud with the finite element method (FEM) the stud is modelled like it is shown in Figure 2 b). The rounded corners were removed, and the weld bead is modeled as illustrated in Figure 2 d). The bead is divided into eight sections and the height is discretized into five portions with a step size of 2 mm. This leads to 390.625 combinations which must been considered for calculating the eigenfrequencies of the different weld conditions.

A first attempt is to use commercial software such as ANSYS to perform a modal analysis on the 3D model mentioned above. The model is meshed and the eigenfrequencies are calculated with FEM. As a volume model is meshed, the resulting nodes and element counts are high. Therefore, the computation time, which is proportional to the number of nodes, is also high. Additionally, the stud must be meshed for every combination of bead section heights. This also leads to high computation time. In conclusion the calculations for all combinations will last too long for an appropriate use in industrial context.
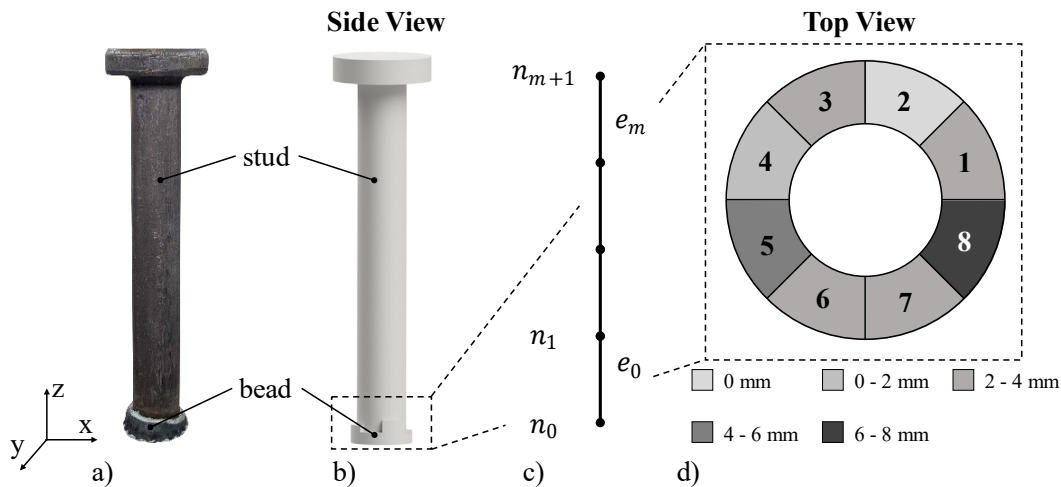

Figure 2: Modeling method for the stud a) Real-world welded stud. b). 3D model of the welded stud with segmented weld bead. c) Model of the new 1D simulation approach with CALFEM. d) Top View of the weld bead segments with section numbers and corresponding bead heights.

To overcome this issue a new modeling strategy is developed in this paper. The stud can be modelled as a 1D beam with varying cross sections in his main axis. This reduces the number of elements drastically and therefore the computation time. Also, the meshing of the stud can be reduced to one initial meshing at the beginning of the calculation process. The resulting model is pictured in Figure 2 d). The element length is chosen to be a multiple of 0.1 mm to fit into the step sizes of the sectioned weld bead.

3. CALCULATION OF THE EIGENFREQUENCY

With CALFEM for Python [10] an appropriate software was found which allows to build up a calculation scheme for the eigenfrequencies with FEM from scratch. To calculate the

eigenfrequencies in 3D the *beam3e* function of CALFEM is used. The function considers different material and geometric parameters as input. In Table 1 the material parameters which kept constant during the calculations are listed. Additionally, the cross-section area A, the moment of inertia with respect to the y axis I_y, the moment of inertia with respect to the x axis I_x, the polar moment of inertia J_t and the St. Venant torsion constant K_v are inputs to the function which returns the stiffness matrix for an element. Except the torsion constant all parameters are calculated with their analytical formulas. In case of the bead sections the areas and moments of inertia are the sum of the inner circle and the arc segments areas.

model parameter	formula sign	value
modulus of elasticity	E	210 MPa
shear modulus	G	81 MPa
density	ρ	7850 kg/m³

Table 1: Model parameters which kept constant during simulation experiments.

The exact formula for the torsion constant is given in equation *(1)*, where ϕ is the torsion angle and A the area of the cross-section. With the external boundary in *(3)* and the internal boundary in *(4)* such that the equation *(2)* is fulfilled. A_e is the area which is enclosed by the internal boundary and n and s are co-ordinate axes normal and tangent to the boundary. With respect to the boundaries *(1)* is only analytically solvable for basic geometries [11]. In *(5)* the formula for a solid circle with radius r is shown. For arbitrary sections only numerical approximative solutions using the finite difference method (FDM) are possible.

$$K_v = 4 * \int_A \phi \, dA \quad (1)$$

$$\frac{\partial^2 \phi}{\partial x^2} + \frac{\partial^2 \phi}{\partial y^2} + 1 = 0 \quad (2)$$

$$\phi = 0 \quad (3)$$

$$\oint \frac{\partial \phi}{\partial n} ds = A_e \quad (4)$$

$$K_v = \frac{\pi * r^4}{2} \quad (5)$$

The cross section is divided into an equally spaced grid of grid size δ. Equation *(6)*, derived from *(2)* and rewritten in terms of FDM terms, takes into account four surrounding points in the grid to calculate ϕ_0. With the condition in *(3)* that the values of ϕ outside the cross sections area are all zero, we can iterate over all cross-section points inside the area until the values converge. Summing up all the values gives the torsion constant.

A ray-casting algorithm is used to check whether a mesh point is in the section. The outer boundaries of the area are approximated as a polygon. Next, a grid point is selected, and a horizontal line is drawn to the right. The number of times the line intersects the outer boundaries is counted. If the number of intersections is odd, the point is inside the boundaries and therefore inside the area. If the number is even, the point is outside the area. By iterating over all the points on the grid, the relevant points that are in the area and need to be calculated are known. The convergence criterion is defined as if the difference between the last calculated torsion constant and the actual one being less than 0.00001 mm^4.

$$\phi_0 = \frac{\phi_1 + \phi_2 + \phi_3 + \phi_4 + \delta^2}{4} \qquad (6)$$

To investigate the effect of the grid size, several experiments are carried out with different grid sizes. For comparison, the torsional constant is calculated for the stud diameter without any bead section. This allows the deviation between the analytical and FDM results to be calculated. The grid space is varied in non-linear distance. Figure 3 b) shows the computation time as a function of the grid space. As excepted, the computational time increases as the grid size decreases. In contrast the deviation from the analytical solution becomes smaller. As a good compromise the grid-space is set to 0.08 mm. The absolute error is 84.32 mm^4, which can be considered as sufficiently accurate.
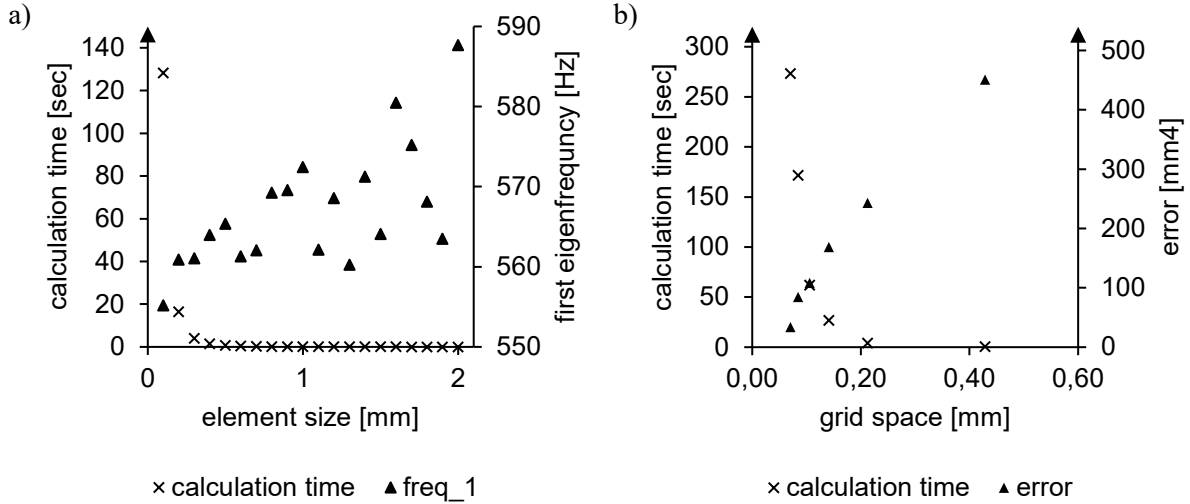

Figure 3: a) Calculation time and values of the first eigenfrequency as a function of the element size of the simulation. b) Calculation time and error of the torsional constant as a function of the element size of the FDM.

Using the calculation scheme described above, a look-up table is calculated for all 256 combinations of weld bead cross sections to be used in modal analysis.

With the equation of motion in *(7)*, the eigenfrequencies can be calculated. With U as the system displacement vector, K as the stiffness matrix of the system and M as the mass matrix of the whole system. Using the standard solution approach for homogeneous linear differential equations with constant coefficients, we obtain an algebraic system of equations. The eigenfrequencies are obtained by evaluating the eigenvalues of the system of equations.

$$M * \ddot{U} + K * U = 0 \qquad (7)$$

Since the CALFEM for Python function *beam3e* only returns the stiffness matrix, the calculation of the mass matrix for a beam element is implemented in the library. For this purpose the approaches of [12] were used and rewritten for use in CALFEM. Due to the fact that the values in the element matrices are somehow sorted, they can be easily assembled and provide a symmetric system stiffness and mass matrix. To solve the eigenvalue problem, the approach used in CALFEM is replaced by a faster algorithm based on LAPACK. This takes advantage of the fact that the matrices are symmetric to obtain faster results.

Taking the boundary condition into account that the stud is fixed at the bottom, the corresponding column and row in the matrices are removed before solving the eigenvalues are calculated.

Like the experiments with the grid space an investigation of the element size for the FEM simulation is carried out. In Figure 3 a) shows a similar behavior to the previous experiments. The computation time decreases as the element size increases. Contrary to the computation

time, the first eigenfrequency decreases with decreasing element size. Again, for the sake of comparison, only the stud without any weld bead is used. In order to generate a complete data set with all possible combinations of weld beads in time, a fast computation time is chosen with an assumed high accuracy of the eigenfrequencies. The calculations in this approach have been performed with an element size of 0.5 mm with a corresponding calculation time of approximately 0.7 seconds for one run. This leads to a total calculation time of 3.164 days for all combinations. All calculations are performed on the same general office personal computer with four kernels. Also, the python code is not optimized, or parallel computation is added. All other libraries used except CALFEM are standard python libraries.

As result the first ten eigenfrequencies are returned and saved in a file. Also, the corresponding segment combination as well as the calculation time for the run are saved.

4. RESULTS & DISCUSSION

To evaluate the new simulation method, the results are compared with the ANSYS simulation. The experiments are performed with the same material properties and the mesh element sizes are varied. Figure 4 shows a similar behaviour to the new approach. However, the element sizes are chosen at higher levels. As the element size increases, the first eigenfrequency decreases. The computation time also decreases with increasing element size, but there is a limit of about 3 seconds that cannot be undercut. The calculation time does not include mesh generation. As the eigenfrequency is only changing in a small range with small element sizes, it is assumed that 555 Hz is the first eigenfrequency.
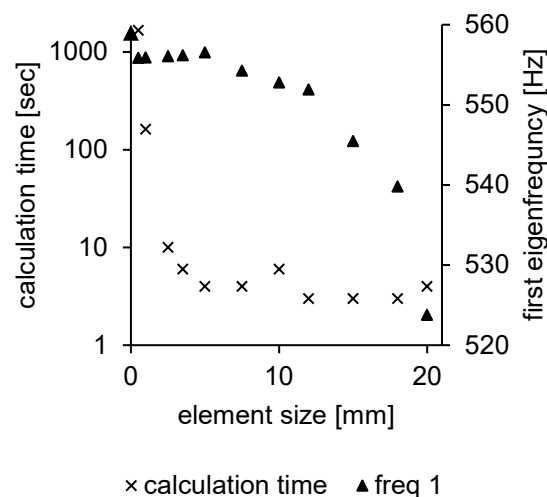

Figure 4:Comparison of different element sizes of the ANSYS simulation in function of the calculation time and the first eigenfrequency

Comparing the new simulation approach with the ANSYS simulation, there is an absolute error of 10 Hz, which corresponds to a relative error of 1.8%. However, the computation time is reduced by a factor of four. Since the error can be expressed as a systematic error and since only the change in the natural frequency is assumed to be relevant for the prediction of the weld bead shape, the error rate can be accepted. To verify the resulting frequency of both simulations real world experiments should be carried out.

Analyzing the obtained results from the simulation the first ten eigenfrequencies have their minimum at 565 Hz and their maximum at 24.976 Hz. The resulting eigenfrequencies accord to the different eigenmodes. The first modes are the bending of the stud. The other ones correspond to the torsional or normal displacements. While the first two eigenmodes have the greatest amplitude they will be analyzed further.

For the first eigenfrequency a mean frequency of 598 Hz can be observed with a standard deviation of 4.6 Hz. For the second eigenfrequency a mean of 601 Hz with a standard deviation of 3 Hz is observed. The variation of the eigenfrequencies is almost very small due to the small geometry changes. In comparison the higher eigenfrequencies like the fourth or the fifth eigenfrequency have a standard deviation of 33.8 Hz or 22.5 Hz with corresponding means of 4189 Hz and 4213 Hz.

It can be clearly seen that to get the weld bead shape in real world applications with the help of the eigenfrequencies a very sensitive system has to be used for measuring the vibration signal and getting the swinging frequencies.

5. CONCLUSION

In this paper, a new method for a fast simulation model is implemented using an existing software suite that has been updated and enhanced with relevant features. An appropriate modelling method has been developed for this purpose. It attempts to map the relevant information of the weld bead to the simulation model. A comparison between commercial simulation software such as ANSYS was also carried out. It was shown that with the chosen element size of 0.5 mm, the new approach makes an error of 10 Hz, but the calculation speed is accelerated by a factor of 4. The resulting eigenfrequencies of the 390,625 combinations of weld bead shapes were analyzed. Small variations were observed, confirming the assumption that eigenfrequencies can be used to predict weld bead shape. However, as a quantified method, a system with high sensitivity to small frequency changes must be used. In order to verify the developed model, real experiments should be carried out. Furthermore, the simulation can be accelerated with a more powerful computer system and an optimized code. This will allow smaller element sizes to be chosen, thus reducing the error.

6. REFERENCES

[1] H.A. Chambers, Principles and Practices of Stud Welding, pcij 46 (2001) 46–58. https://doi.org/10.15554/pcij.09012001.46.58.

[2] DIN EN ISO 14555:2017-10, Schweißen - Lichtbogenbolzenschweißen von metallischen Werkstoffen (ISO_14555:2017); Deutsche Fassung EN_ISO_14555:2017, Beuth Verlag GmbH, Berlin.

[3] J. Dong, G. Xu, H. Yu, G. Fan, L. Wei, X. Gu, Connection status evaluation in arc stud weld joints by ultrasonic detection, Int J Adv Manuf Technol 100 (2019) 663–672. https://doi.org/10.1007/s00170-018-2752-9.

[4] N.K.A. Al-Sahib, H.K.A. Ameer, S.G.F. Ibrahim, Monitoring and quality control of stud welding, Al-Khwarizmi Engineering Journal 5 (2009) 53–70.

[5] S. Naddaf Shargh, M. Naddaf-Sh, M. Dalton, S. Ramezani, A.R. Kashani, H. Zargarzadeh, Explainable Models for Multivariate Time-series Defect Classification of Arc Stud Welding, IJPHM 14 (2023). https://doi.org/10.36001/ijphm.2023.v14i3.3125.

[6] I. Samardžić, Z. Kolumbić, Š. Klarić, Welding parameter monitoring during stud arc welding, Pollack Periodica 4 (2009) 29–39. https://doi.org/10.1556/Pollack.4.2009.1.4.

[7] I. Samardžić, D. Žagar, S. Klaric, S. Fakultet, U. Slavonskom, B. Sveučilišta, J. Strossmayera, Osijeku, Elektrotehnički, O. Sveučilišta, I. Hr, Application and Upgrading of On-line Monitoring System for Measurement and Processing of Electric Signals at Arc Stud Welding Process, Strojarstvo 517917882 (2009) 355–363621.

[8] E. Damerow, Die praktische Werkstoffabnahme in der Metallindustrie, Springer Berlin Heidelberg, Berlin, Heidelberg, 1935.

[9] DIN EN ISO 13918:2021-12, Schweißen – Bolzen und Keramikringe für das Lichtbogenbolzenschweißen (ISO 13918:2017 + Amd 1:2021); Deutsche Fassung EN ISO 13918:2018 + A1:2021, Beuth Verlag GmbH, Berlin.

[10] CALFEM for Python, 2022.

[11] S.P. Timošenko, J.N. Goodier, Theory of elasticity, 3rd ed., McGraw-Hill, Auckland, 2004.

[12] B. Klein, FEM: Grundlagen und Anwendungen der Finite-Element-Methode im Maschinen- und Fahrzeugbau, 10th ed., Springer Vieweg, Wiesbaden, 2015.

CONTACTS

Maximilian Rohe

email: maximilian.rohe@tu-ilmenau.de
ORCID: https://orcid.org/0000-0003-4621-2458